

IGF-1 Expression in Infarcted Myocardium and MGF E Peptide Actions in Rat Cardiomyocytes *in Vitro*

Anastasia Stavropoulou,¹ Antonios Halapas,¹ Antigone Sourla,² Anastassios Philippou,¹ Efstathia Papageorgiou,¹ Apostolos Papalois,³ and Michael Koutsilieris¹

¹Department of Experimental Physiology, Medical School, National Kapodistrian University of Athens, Goudi-Athens, Greece;

²Endo/OncoResearch Medical Laboratories, Ampelokipi, Athens, Greece; ³ELPEN Research Center, Animal Research Facility Unit, Palini, Attiki, Greece

Insulinlike growth factor-1 (IGF-1) expression is implicated in myocardial pathophysiology, and two IGF-1 mRNA splice variants have been detected in rodents, IGF-1Ea and mechano-growth factor (MGF). We investigated the expression pattern of IGF-1 gene transcripts in rat myocardium from 1 h up to 8 wks after myocardial infarction induced by left anterior descending coronary artery ligation. In addition, we characterized IGF-1 and MGF E peptide action and their respective signaling in H9C2 myocardial-like cells *in vitro*. IGF-1Ea and MGF expression were significantly increased, both at transcriptional and translational levels, during the late postinfarction period (4 and 8 wks) in infarcted rat myocardium. Measurements of serum IGF-1 levels in infarcted rats were initially decreased (24 h up to 1 wk) but remained unaltered throughout the late experimental phase (4 to 8 wks) compared with sham-operated rats. Furthermore, specific anti-IGF-1R neutralizing antibody failed to block the synthetic MGF E peptide action, whereas it completely blocked IGF-1 action on the proliferation of H9C2 cells. Moreover, this synthetic MGF E peptide did not activate Akt phosphorylation, whereas it activated ERK1/2 in H9C2 rat myocardial cells. These data support the role of IGF-1 expression in the myocardial repair process and suggest that synthetic MGF E peptide actions may be mediated via an IGF-1R independent pathway in rat myocardial cells, as suggested by our *in vitro* experiments.

© 2009 The Feinstein Institute for Medical Research, www.feinsteininstitute.org

Online address: <http://www.molmed.org>

doi: 10.2119/molmed.2009.00012

INTRODUCTION

Myocardial infarction occurring after coronary artery occlusion leads to ischemic injury-mediated necrosis of myocardium followed by subsequent redistribution of cardiac loading in the viable myocardial tissue, which could result in congestive heart failure (CHF). CHF is considered to be an irreversible process, a belief stemming from the assumption that cardiac cells are not able to regenerate (1,2). Recent data suggest, however, that myocardium regenerates and that growth factors, such as insulinlike growth factor-1 (IGF-1), may play an im-

portant role in this process by preventing the apoptosis of myocardial cells (3–7).

The *IGF-1* gene consists of six exons, and alternative splicing has led to the identification of two different mRNA transcripts in rodents (8), IGF-1Ea and mechano-growth factor (MGF). IGF-1Ea is the main isoform produced by the liver under the control of growth hormone (GH), and MGF was initially detected in skeletal muscle and was shown to be significantly upregulated by mechanical stimulation (9). The MGF splice variant differs from IGF-1Ea by a 52-bp insert within the E domain of exon 5.

This insert results in a translational frame shift that leads to a carboxy terminal sequence different from that of IGF-1Ea (8). Thus, two IGF-1 precursor polypeptides are raised from the different *IGF-1* transcripts. These IGF-1 propeptides yield the same mature IGF-1 peptide, which is derived from the highly conserved exons 3 and 4 of the *IGF-1* gene. These exons are known to code for the binding domain of the IGF-1 receptor (IGF-1R). Posttranslational cleavage of IGF-1 precursor polypeptides removes the signal and the E-peptide and results in different E domains (10,11).

We examined the endogenous expression of IGF-1Ea and MGF after artery ligation-induced myocardial infarction in rats, and we characterized MGF E peptide signaling in H9C2 myocardial-like cells using a synthetic peptide that contained the last 24 amino acids of the E domain. Our data suggest that in rat

Address correspondence and reprint requests to Michael Koutsilieris, Department of Experimental Physiology, Medical School, National and Kapodistrian University of Athens, Micras Asias 75, Goudi-Athens, 11527, Greece. Phone: +30-210-7462597; Fax: +30-210-7462571; E-mail: mkoutsil@med.uoa.gr.

Submitted March 5, 2009; Accepted for publication March 6, 2009; Epub (www.molmed.org) ahead of print March 6, 2009.

myocardium, IGF-1 transcript expression is upregulated during the late postinfarction period, whereas in rat myocardial cells *in vitro*, MGF E peptide exerts autonomous, IGF-1R-independent action.

MATERIALS AND METHODS

Experimentally Induced Myocardial Infarction in Rats

For this investigation we used 72 male Wistar rats weighing 280–330 g. The study protocol was approved by the local ethics committee. Animals were housed 1–3 per cage in an approved animal facility (ELPEN Pharmaceuticals, Athens, Greece) with 12:12 h light-dark cycles and given free access to standard rodent chow and water. Before surgery rats were put under ether anesthesia in a specifically designed box for about 2 to 3 min. Subsequently, endotracheal intubation was performed under laryngoscopy by a specifically trained investigator and research assistant with the use of a 16-G venous catheter connected to a rodent ventilator (Harvard Apparatus, Holliston, MA, USA) at the following settings: tidal volume, 3 mL; rate, 70 breaths/min. Proper intubation was confirmed by observation of chest expansion and retraction during ventilated breaths. Anaesthesia was maintained using a mixture of 93% O₂, 5% CO₂, and 2% isoflurane. Myocardial infarction was induced by proximal artery ligation of the left anterior descending coronary artery as previously described in detail (12). Briefly, after left thoracotomy the pectoralis muscle groups were dissected or cut transversely, exposing the thoracic cage. Occasionally, the internal mammary artery was severed, but bleeding usually stopped spontaneously. Blunt curved forceps were then plunged between the fifth and sixth ribs, through the intercostal muscles, at a point approximately 2 mm to the left of the sternum. In this way, bleeding from the internal epigastric artery was avoided. The gap was then widened by gentle pressure with the perforating forceps, and then the sixth rib was transacted with scissors. Bleeding

that occurred occasionally was stopped with application of pressure with a sterile cotton swab for <20 s. With the use of forceps the pericardium was disconnected. A 6-0 silk suture (Ethicon, Somerville, NJ, USA) placed at the apex of the heart enabled us to exteriorize it without difficulty. We then introduced the needle of a 6-0 silk suture (Ethicon) into the pulmonary cone and brought it to the surface again at a point near the insertion of the left atrial appendage. In that way, the left coronary artery was ligated near its origin, producing a large myocardial infarction. By following these anatomical landmarks we were able to accurately reproduce the infarct size. Then, the heart was placed back into the thorax and the intercostal muscles were tightened to close the thoracic wall. Slight lateral pressure after tying this ligature squeezed the air out of the thorax, and because the skin, subcutaneous tissue, and muscles act as a valve, the pneumothorax was evacuated. The animals regained consciousness soon after we stopped the administration of isoflurane. The mortality due to the surgical procedure was 18% in our hands. Sham-operated animals were used as controls. In these animals the same procedure was followed without the ligation step. Animals were killed after the ligation procedure according to the protocol (at 1 h, 24 h, 4 d, 8 d, 4 wks, and 8 wks postsurgery).

Infarct size was confirmed by use of the Tetrazolium method. Briefly, in the anesthetized rat, the heart was excised and cut from apex to base transversely in sections 2-mm thick. The sections were then incubated in a 1% solution of triphenyltetrazolium chloride (TTC) for 10 to 15 min until viable myocardium was stained brick red. Infarct-related myocardium is not stained with TTC. The tissue sections were then fixed in a 10% formalin solution and weighed. Color digital images of both sides of each transverse slice were obtained. The infarct zone and the periinfarct area were determined on the basis of the observed size of the infarct (~40% of the myocardium) and on

the indicative tissue sections stained with TTC.

RNA Extraction and Reverse Transcription-Polymerase Chain Reaction Conditions

The rat cardiac tissues were homogenized (Ultra-Turrax T25; Thermo Fisher Scientific, Cheshire, UK) at 500g, and total RNA was extracted according to the Trizol Reagent protocol (Invitrogen, Carlsbad, CA, USA). Diethylpyrocarbonate-treated water was used for the dilution of the RNA pellet. The RNA concentration was estimated spectrophotometrically (Genova; Jenway, Essex, UK) by absorbance at 260 nm and the purity by the ratio of the absorbance at 260/280 nm. The RNA integrity was assessed by visualization of the 18S and 28S ribosomal RNA pattern in a denaturing agarose gel. In each sample 2 µg of total RNA was reverse-transcribed into cDNA by use of SuperScript II reverse transcriptase (Invitrogen) as described previously (13).

To study the relative mRNA expression of the IGF-1Ea and MGF, in each polymerase chain reaction (PCR) reaction every target cDNA was coamplified with classic 18S internal standard (detected at 489 bp) (Ambion, Austin, TX, USA), and its expression was given as a ratio of the target cDNA/18S. This procedure compensates for differences in starting amounts of total RNA and in reverse transcription (RT) efficiency.

A linearity test for the coamplification of 18S and the different IGF-1 cDNAs (that is, reverse-transcribed mRNAs of MGF and IGF-1 Ea) as a function of PCR cycle number was used to validate the use of 18S for the correction for potential variability in the starting amount of cDNA in each case and to choose the appropriate amplification cycle number. Regression analysis showed that amplification of each PCR product was highly linear for the range of cycles (35–39) tested, with high coefficients of determination (data not shown).

To decrease the 18S signal so as to attain a linear amplification of each target mRNA and 18S to the same range, 18S

primers and antagonists of primers were mixed at ratios that ranged from 1:2 to 1:4 depending on the abundance of the target mRNA. For both controls and pathological samples of every group, the same premixed reagents were used to minimize the differences in PCR efficiency. The relative quantitative RT-PCR methods used in the present study have been extensively validated in previously reported studies (14,15).

The PCR products were measured by use of a relative quantification procedure as described below. Ethidium bromide-stained 2% agarose gels were captured under ultraviolet light in a Kodak EDAS 290 imaging system (Carestream Health, Rochester, NY, USA), and PCR products were quantified by band densitometry with image software (Scientific Imaging Systems, Kodak ID, New Haven, CT, USA). Values of MGF and IGF-1 Ea PCR products were normalized to each corresponding ribosomal 18S and expressed as fold of change from the values of controls.

Primer sequences for rat IGF-1Ea and MGF mRNA were specifically designed on the basis of their specific sequence (8). For IGF-1Ea primers the specific sequences were forward GCTTGCTCAC CTTTACCAGC and reverse AAGTG TACTTCCTTCTGAGTCT; for MGF they were forward GCTTGCTCACCTTACCAGC and reverse AAGTG TACTTCCTTCTC. Primers were designed with the Primer Select computer program (DNASar, Madison, WI, USA) and prepared by Invitrogen. Each set of primers was designed to detect and amplify specifically only one of the IGF-1 isoforms. The PCR mix for the amplification was constructed according to the HotStartTaq DNA Polymerase Kit (Qiagen, Valencia, CA, USA), and the reactions were carried out in a PTC-200 Peltier Thermal Cycler, (MJ Research, Waltham, MA, USA) at annealing temperatures of 65°C for IGF-1Ea and 57°C for MGF and extension at 72°C. The reaction was accomplished after 37 cycles, according to the results of linearity tests for each target mRNA and 18S. The expected

sizes of the specific PCR products were initially verified by electrophoretic separation on agarose gel, and all target sequences were identified by sequencing analysis to ensure specificity of the primers and to further verify each target mRNA. In preliminary experiments, each primer set was tested for its compatibility with the 18S Classic primers.

Protein Extracts and Western Analysis

Total proteins were obtained from rat myocardium by lysis of 10 mg of the tissue in 1 mL RIPA Buffer (50 mM Tris-HCl, 150 mM NaCl; Sigma, St. Louis, MO, USA) containing 0.55 Nonidet P-40; protease inhibitors 1 mM phenylmethylsulfonyl fluoride (Sigma), 10 µg/mL aprotinin, and 10 µg/mL leupeptin (Sigma); and phosphatase inhibitors 1 mM sodium orthovanadate and 1 mM NaF (Sigma). The samples were homogenized (homogenizer Ultra-Turrax T25, Thermo Fisher Scientific, Cheshire, UK) in the RIPA buffer and then incubated on ice for 20 min. The homogenates were cleared by centrifugation (500g, 4°C, 30 min). The extract was stored at -80°C. Protein concentrations were determined by protein assay (Bio-Rad Laboratories, Hercules, CA, USA).

Equal amounts of protein extracts (30 µg) from the myocardial tissues were mixed with a loading buffer [62.5 mM Tris, pH 6.8, 5% glycerol (v/v), 1% SDS (v/v), 2.5% β-mercaptoethanol (v/v)], denatured at 95°C for 4 min, electrophoresed on 16% SDS-PAGE under denaturing conditions, and transferred onto nitrocellulose membrane (Bio-Rad Laboratories). Blots were then incubated with a blocking solution containing 5% nonfat milk powder in Tris phosphate-buffered saline (TBS; 10 mM Tris, pH 7.6; 100 mM NaCl) plus Tween (0.1% Tween 20) (TBS-T) at room temperature for 1 h. After three washes with TBS-T for 10-min intervals, blots were incubated with the following primary antibodies for the immunodetection of IGF-1Ea and MGF proteins: IGF-1Ea, mouse monoclonal anti-IGF-1 (1:200 dilution) (MS-1508; NeoMarkers, Fremont, CA, USA) (molec-

ular weight of antigen, ~21 kDa), MGF, and rabbit anti-human MGF polyclonal antibody (1:10,000 dilution), which was raised against a synthetic peptide corresponding to the last 24 amino acids of the E domain of human MGF, as previously described (16). Blots were incubated with the primary antibodies diluted in TBS-T overnight at 4°C under gentle shaking. After three washes with TBS-T, membrane was incubated with a horseradish peroxidase-conjugated secondary antirabbit IgG (goat antirabbit, 1:2000 dilution; Santa Cruz Biotechnology, Santa Cruz, CA, USA) or antimouse IgG (goat antimouse, 1:2000 dilution; Santa Cruz Biotechnology) in TBS-T containing 1% nonfat milk powder, for 1 h at room temperature. The expected bands were visualized by exposure of the membrane to x-ray film after incubation with an enhanced chemiluminescent substrate for 3 min (SuperSignal; Pierce Biotechnology, Rockford, IL, USA). Glyceraldehyde 3-phosphate dehydrogenase (*GAPDH*, housekeeping gene) (1:2,000 dilution; Santa Cruz Biotechnology) was used as an internal standard to minimize the differences in the loading of the protein. The films were captured under white light in a Kodak EDAS 290 imaging system, (Carestream Health) and proteins were quantified by band densitometry using image software (Scientific Imaging Systems).

Cell Cultures

H9C2 rat myocardial cells were obtained from the American Type Cell Culture (ATCC, Bethesda, MD, USA). H9C2 cells were seeded in 6-well plate in Dulbecco's modified Eagle's medium/F-12 (Cambrex, Walkerville, MD, USA) supplemented with 10% heat-inactivated fetal bovine serum (FBS; Biochrom, Berlin, Germany) and 100 U/mL penicillin/streptomycin (Cambrex) at 37°C in a humidified atmosphere of 5% CO₂. Twenty-four h prior to various treatments, the culture medium was changed to 5% FBS. To study the actions of MGF and IGF-1 in rat myocardium, we used a synthetic peptide comprising the last 24

amino acids of the MGF E domain (16), and a 70-amino acid human recombinant IGF-1 corresponding to the mature IGF-1 peptide (rhIGF-1; Chemicon, Temecula, CA, USA). The synthetic MGF E peptide was synthesized and validated as previously described (16). Both the synthetic MGF E and the mature IGF-1 peptides were used in the following concentrations: 5, 25, and 50 ng/mL for 48 h. In the control cultures, H9C2 cells were treated under the same procedure using phosphate-buffered saline (PBS). To investigate if IGF-1 and MGF peptide act on myocardial cells via IGF-1R signaling, H9C2 cells were incubated with a monoclonal anti-IGF-1R neutralizing antibody (R&D Systems, Minneapolis, MN, USA) for 1 h prior to the various treatments with either mature IGF-1 or MGF peptide. The IGF-1R neutralizing antibody was used at a concentration of 10 µg/mL, according to the manufacturer's recommendation. In these experiments, control wells were treated only with anti-IGF-1R antibody, and the same procedure as in the treatment cultures was followed. H9C2 cells were plated at a cell density of 3.5×10^4 cells/well in 6-well plates and grown with DMEM/F-12 containing 10% FBS. After 24 h of cell seeding, the culture medium was changed to 5% FBS, and the cell cultures were exposed to the appropriate growth factor using dose-dependent experiments. Trypan blue assays were used for a cell number analysis as described previously (17).

To further investigate whether the mature IGF-1 and the MGF E peptide act through different intracellular pathways, we analyzed the activation (phosphorylation) of extracellular regulated kinase 1 and 2 (ERK1 and ERK2) and Akt-kinase (protein kinase B) in H9C2 cells as described previously (18). Briefly, cells were exposed to 50 ng/mL of mature IGF-1 and MGF peptide for 5, 15, 30, and 60 min. Equal amounts of cell lysates (20 µg) were heated at 95°C for 5 min, electrophoresed on SDS-PAGE under denaturing conditions, and transferred onto nitrocellulose membrane (Bio-Rad

Laboratories). The membranes were probed overnight with primary phospho-specific antibodies against phospho-ERK1/2 (Thr 202/Tyr 204), ERK1/2, phospho-Akt (Ser 473) and Akt (1:1,000 dilution; Cell Signaling, Beverly, MA, USA). The blots then were incubated with a secondary goat antibody raised against rabbit IgG conjugated to horseradish peroxidase (1:2,000 dilution; Santa Cruz Biotechnology), and the bands were visualized and densitometrically analyzed.

Serum IGF-1 Determination

The IGF-1 serum concentrations were measured with a commercially available standard sandwich enzyme-linked immunosorbent assay kit, according to the manufacturer's instructions (Immunodiagnostic Systems, Fountain Hills, AZ, USA). The method incorporated a sample pretreatment to avoid interference from binding proteins. A monoclonal anti-IGF-1 antibody was coated onto the inner surface of the microtiter wells. The pretreated, diluted samples were incubated together with biotinylated polyclonal rabbit anti-IGF-1 antibody and shaken for 2 h at room temperature. Then, the wells were washed and horseradish peroxidase-labeled avidin was added and bound to the biotin complex. After an additional wash, a single-component chromogenic substrate was added to develop color. The absorbance of the stopped reaction mixture was read at 450 nm in a microtiter plate reader (Versamax; Molecular Devices, Sunnyvale, CA, USA). All samples were run simultaneously and analyzed in triplicate, and the results were averaged. The sensitivity, defined as the concentration corresponding to the mean plus 2 standard deviations (SD) of 20 replicates of the zero calibrator was 63 ng/mL. IGF-1 serum levels were measured both in experimental and sham-operated rats.

Immunohistochemistry

Myocardial tissues were fixed in 4% formaldehyde, embedded in paraffin

wax, and cut in 3-µm sections. Then, the sections were adhered to glass slides, dried at 37°C overnight, dewaxed in xylene, and rehydrated in serial dilutions of ethanol. Then, the sections were immersed in 1% hydrogen peroxide in distilled water for 15 min and washed in distilled water and PBS buffer. Finally, the sections were incubated with the same primary polyclonal anti-MGF antibody that was used for the Western blot assay (at a dilution of 1:1000), in PBS overnight at 4°C. After washing in PBS buffer, secondary biotinylated goat antirabbit IgG (Dako Real EnVision, Glostrup, Denmark) was added for 25 min at room temperature, followed again by repeated PBS buffer washes. Incubation of the sections in a solution of 3,3'-diaminobenzidine substrate-chromogen (Dako Real EnVision) in PBS (for 10 min) enabled the visualization of the immunocomplex. Staining was accomplished by immersion in hematoxylin for 5 min. After being washed in distilled water the sections were dehydrated in serial dilutions of ethanol and xylene and finally mounted in dibutyl phthalate xylene. The visualization of the sections was accomplished with a PENTAX-ZX-50 ASAHI digital color camera mounted on the microscope. The same experimental procedure was also performed for the negative control samples, with the omission of the primary antibodies.

Statistical Analysis

Changes in cell number analyses and in the transcriptional and translational expression of IGF-1 isoforms, as well as changes in IGF-1 serum measurements, were assessed using two-way analysis of variance with repeated measures over time (SPSS v. 11 statistical package). When significant F ratios were found for main effects or interaction ($P < 0.05$), the means were compared using Tukey's post-hoc tests. All data are presented as mean \pm standard error of the mean (SEM). The level of significance was set at $P < 0.05$.

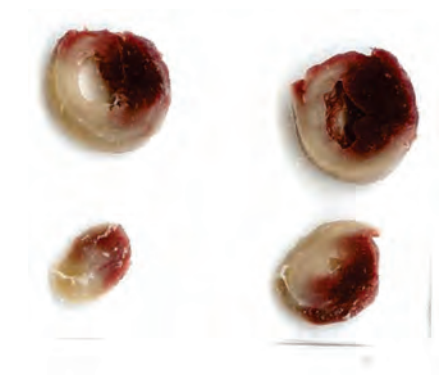


Figure 1. Histopathological analysis of the size of the infarcted region in rat myocardium using the Tetrazolium (TTC) method. Viable myocardium was stained brick red, whereas infarcted myocardium failed to be stained with TTC. In our experiments, 20%–40% of the rat myocardium was apparently damaged. Presented here is an example of rat myocardium excised and cut from base (upper panel) to apex (lower panel) transversely in 2-mm thick sections and stained with TTC.

RESULTS

Infarct Evaluation and IGF-1 Expression after Myocardial Infarction

In all experimental animals, ligation of the left anterior descending artery did provoke an infarct, which extended from 20% to 40% of the rat myocardium (viable myocardium was stained brick red, whereas infarcted myocardium failed to be stained with TTC; Figure 1). In each animal the infarction was confirmed initially by the cyanotic color of the injured myocardium and by the deviation of the electrical axis in the electrocardiogram (data not shown). The expression of IGF-1Ea and MGF was documented both at the transcriptional and translational levels using PCR, Western blot, and immunohistochemical analysis (Figure 2). The expression profiles of IGF-1Ea and MGF during the postinfarction period revealed that both IGF-1Ea and MGF expression were significantly increased at 4 and 8 wks postinfarction in rat myocardium. However, fold increase of MGF expression was significantly higher (greater

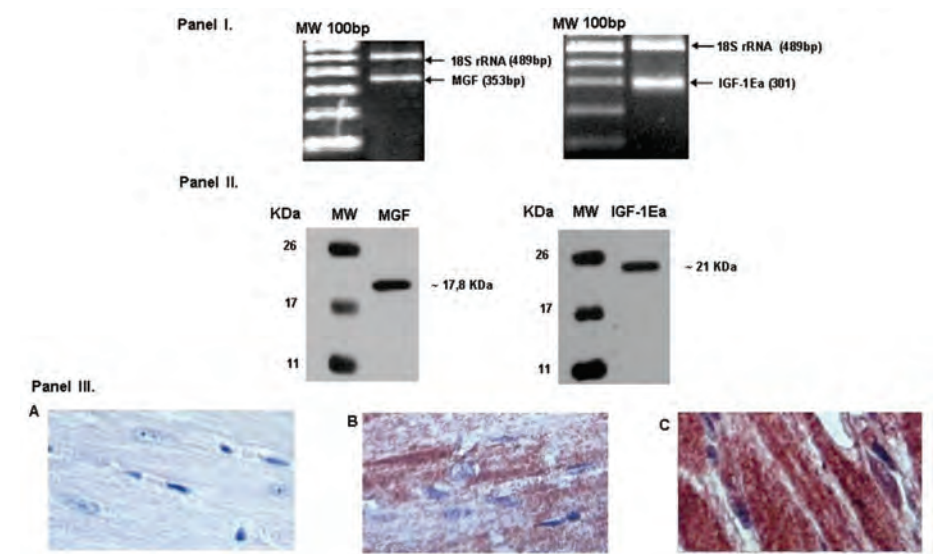


Figure 2. Expression of the IGF-1 isoforms in rat myocardium. Panel I: Specific PCR products for MGF and IGF-1Ea mRNA detected in rat myocardium. The PCR products were confirmed by sequencing. Panel II: Detection of MGF and IGF-1Ea at the protein level using Western blot analysis. Panel III: Photomicrographs (magnification, $\times 40$) of the left ventricular sections of rat myocardium stained with anti-MGF antibody. Specificity of the immunohistochemical MGF detections was confirmed by the absence of immunoreactivity in the negative control sections (A). Note that myocardial tissues of sham-operated rats appear less intensively stained (B) compared with infarcted tissues (C).

than five-fold) than that of IGF-1Ea (two-fold) at both the transcriptional (Figure 3, panel I) and translational level (Figure 3, panel II).

Serum IGF-1 levels measured in the infarcted animals were significantly decreased compared with those of the sham-operated animals at the early postinfarction period (24 h and 8 d postinfarct) (Figure 4). Throughout the experimental period, however, measured levels were not significantly different in experimental animals compared with those measured in sham-operated animals (Figure 4; $P > 0.05$).

Characterization of Mature IGF-1 and Synthetic MGF E Peptide Actions on H9C2 Cell Proliferation

Trypan blue exclusion assays revealed that the synthetic MGF E peptide stimulated the proliferation of H9C2 cells as it did mature IGF-1 (Figure 5, panel I). However, the action of the synthetic MGF E peptide of H9C2 cells was not blocked by the anti-IGF-1R neutralizing antibody.

In contrast, anti-IGF-1R neutralizing antibody completely blocked the IGF-1-mediated action on H9C2 cells, suggesting that synthetic MGF E peptide action was mediated by an IGF-1R-independent mechanism (Figure 5, panel I). Exogenous administration of mature IGF-1 produced a time-dependent increase of ERK1/2 and Akt phosphorylation in H9C2 cells (Figure 5, panel II). However, the synthetic MGF E peptide activated ERK1/2 without affecting Akt phosphorylation (Figure 5, panel II). These data reinforced the notion that MGF E peptide acts on H9C2 cells through IGF-1R-independent signaling.

DISCUSSION

IGF-1 actions are mediated via the type I IGF-1 receptor (IGF-1R) (19). However, insulin receptor (IR) and the hybrid IGF-1R/IR were recently reported to mediate certain IGF-1 actions (20). Two primary signaling pathways are associated with the activation of IGF-1R (21,22). The Raf-MEK-ERK signaling pathways are

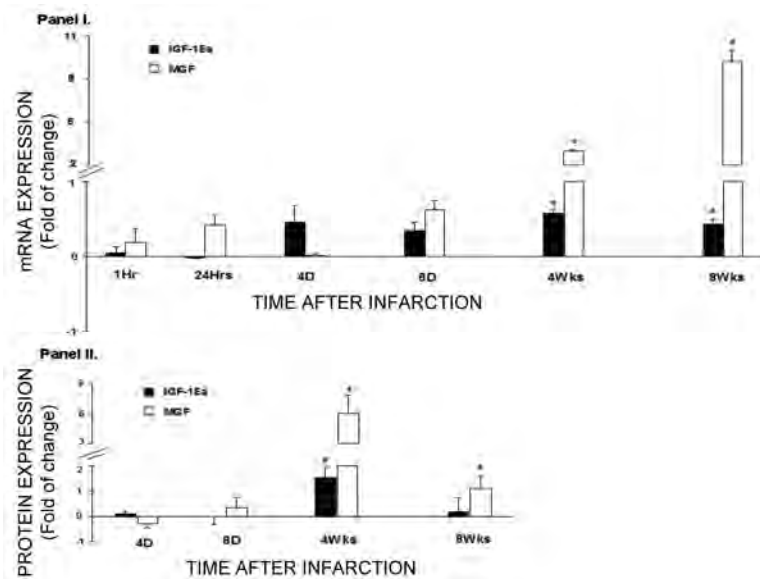


Figure 3. Panel I: mRNA expression of IGF-1Ea and MGF splice variants at different time points after experimental occlusion of the left descending coronary artery. Bars represent mean values (mean ± SEM of six measurements) of respective mRNA expression, which was normalized to each corresponding ribosomal 18S and expressed as the fold change of the mRNA levels in sham-operated rats (controls). PCR amplification for both 18S and the different IGF-1 transcripts was in linear phase at 37 cycles at all time points. *Statistically significant values: $P < 0.05$. Panel II: Expression of IGF-1Ea and MGF at the protein level using Western blot analysis. Immunoblotting for GAPDH served as a control for protein loading. Expression values (means ± SEM of six measurements) were normalized to those of corresponding GAPDH in the same immunoblot and expressed as the fold change of the sham-operated rats (controls). *Statistically significant values: $P < 0.05$.

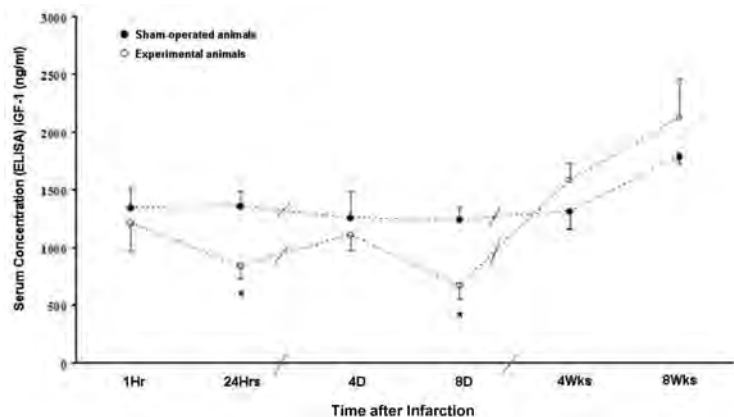


Figure 4. Serum IGF-1 levels measured in sham-operated and infarcted rats using enzyme-linked immunosorbent assay as described in the “Material and Methods” section. Concentrations of IGF-1 were expressed as mean ± SEM of six measurements. * $P < 0.05$. Note that IGF-1 serum levels were decreased early (1 h to 1 wk) during the experimental procedure; however, these levels were not different during the late phase (4 wks and 8 wks) of the experimental procedure compared with measurements in sham-operated rats.

linked to cell growth and proliferation (21,23), and the activation of the phosphatidylinositol 3-kinase (PI3K)-Akt signaling cascade is critical for cell metabolism, growth, and antiapoptotic responses (24).

Interest has recently increased in the role of the IGF-1 isoforms in the regulation of cardiac cell survival and function after myocardial infarction (25). Exogenous administration of a synthetic MGF E peptide reduced postinfarct apoptosis in the periinfarct zone of sheep myocardium (12,25). In addition, genome-wide analysis in rats revealed upregulation of IGF-1 postinfarction (26). Indeed, our data corroborate these data because coronary artery ligation-induced myocardial infarction was followed by an endogenous increase of IGF-1Ea and MGF expression, both at mRNA and protein levels. This finding was evident at the late postinfarction period (4 weeks and 8 weeks postinfarction), which is known to correspond to the timing of the cardiac remodelling/repair process in the postinfarction period (27–30). Notably, in a genome-wide (microarray) analysis in mice, up to 48 hours after myocardial infarction, IGF-1Ea and MGF were not reported to be detected (31).

Our data also reveal legitimate evidence to support the notion that biologic actions and signaling of the synthetic MGF E peptide are mediated via an IGF-1R-independent mechanism. Conceivably, both IGF-1Ea and MGF expression play a role in the pathophysiology of rat myocardium; however, proteolytic production of the MGF E peptide by the MGF transcript apparently generates a novel mitogen for rat myocardial cells, which possesses possibly autonomous biologic actions.

The upregulation of IGF-1 expression, documented in our study, is in concert with recently reported findings of previous studies indicating that myocardial hypertrophy after infarction is accompanied by a progressive increase in cardiomyocyte volume over time (32), an adaptive mechanism (29,33,34) that involves IGF-1 expression (35,36). IGF-1

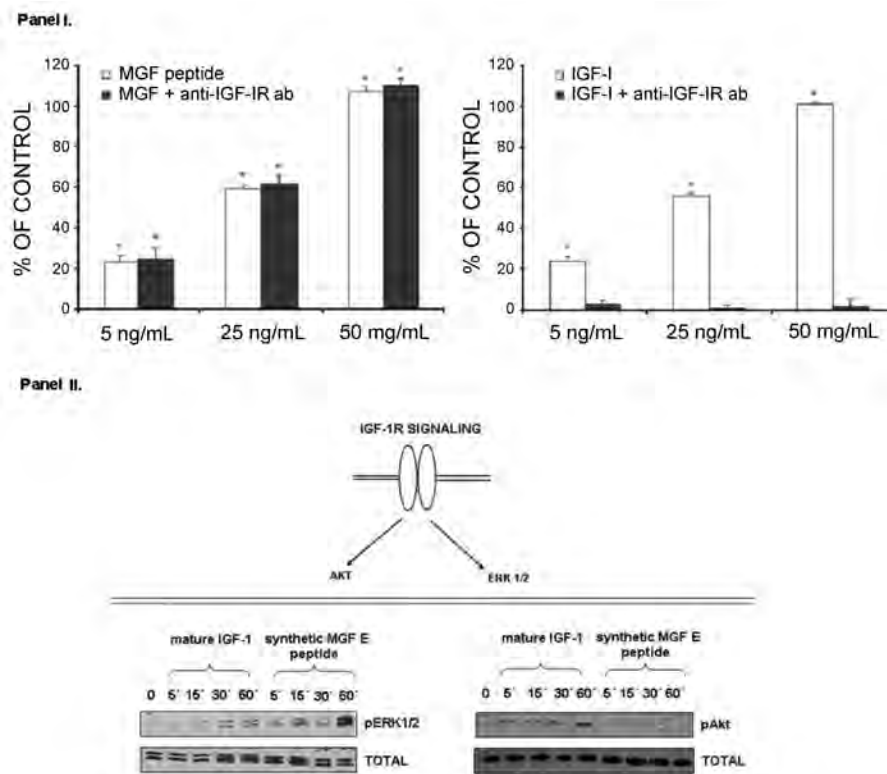


Figure 5. Analysis of H9C2 cell proliferation using the trypan blue assay. Panel I: The effects of mature IGF-1 and synthetic MGF E peptide on H2C2 cell proliferation (% cell number changes) in a dose-dependent manner as presented in the “Materials and Methods” section. Note that the IGF-1R neutralizing antibody (anti-IGF-1R ab) blocked IGF-1 effects without affecting the action of synthetic MGF E peptide on H9C2 cell proliferation. Data are presented as mean \pm SEM. *Significantly different ($P < 0.001$) from control conditions. Panel II: Representative Western blot analysis of ERK1/2 and Akt phosphorylation in H9C2 cells after stimulation with IGF-1 and synthetic MGF E peptide in a time-dependent manner. Note that the MGF E peptide activated ERK1/2 phosphorylation; however, it did not activate Akt phosphorylation. IGF-1 did activate both ERK1/2 and Akt in H9C2 myocardial-like cells as expected. These data suggest that synthetic MGF E peptide could signal via an IGF-1R-independent mechanism in H9C2 cells.

has been consistently reported to mediate skeletal muscle hypertrophy (21,36,37), myocardial cell survival, and myocardium repair and hypertrophy (5,38–43). In particular, IGF-1 expression prevented apoptosis of the viable myocardium after infarction and was implicated subsequently in cardiac hypertrophy and its detrimental impact on heart function (5,38,44). The two major IGF-1R-mediated signaling pathways, namely the Raf-MEK-ERK and the PI3K-Akt pathways, were both shown to be activated in myocardium postinfarction (45–47). Indeed, the PI3K-Akt pathway was implicated in the survival of cardiac

myocytes and protection of myocardial cells from reperfusion-induced injury in both *in vitro* (45,48) and *in vivo* studies (49). In addition, the IGF-1R-PI3K-Akt signaling pathway was shown to be essential for myocardial hypertrophy (50–52). However, the data on the role of ERK phosphorylation in cardiac hypertrophy vary substantially. There is evidence that ERKs are involved as immediate downstream effectors of the cardiomyocyte hypertrophic responses (34,53) without being the sole mediators of such responses (54). Moreover, evidence indicates that activation of ERKs may have an inhibitory effect on hyper-

trophic responses (55–57). Our study has evaluated the endogenous transcriptional and translational expression of the IGF-1 isoforms after myocardial infarction, showing that the fold increase of MGF expression was higher than that of IGF-1Ea. Thus, we postulate that increased MGF expression during this period could be a key determinant during the late postinfarction period, reflecting possibly local needs for a selective increase of ERK1/2 phosphorylation in infarcted myocardium.

Therefore, we propose that the upregulation of IGF-1Ea and MGF in the late postinfarction period *in vivo* could participate in the repair processes via IGF-1R-mediated and IGF-1R-independent mechanisms.

Notably, the upregulation of endogenous IGF-1 expression in rat myocardium was not accompanied by an increase of measured IGF-1 levels in serum, supporting the notion that IGF-1 expression serves the needs of rat myocardium locally.

In conclusion, we have documented that there is an increase of IGF-1 expression in rat myocardium after coronary artery infarction. The actions of our synthetic MGF E peptide are possibly IGF-1R independent, based on our *in vitro* studies using this synthetic MGF peptide. However, it would be interesting to test whether *in vivo* experiments can verify this type of action *in vivo* for the naturally occurring MGF E peptide. Elucidation of the precise role of MGF E peptide actions in cardiac repair and hypertrophic responses of the myocardium requires further investigation. In particular, the possible role of IGF-1 transcripts in other pathophysiological conditions (58–63) requires further investigation.

DISCLOSURE

We declare that the authors have no competing interests as defined by *Molecular Medicine*, or other interests that might be perceived to influence the results and discussion reported in this paper.

REFERENCES

- Anversa P, Li P, Zhang X, Olivetti G, Capasso JM. (1993) Ischaemic myocardial injury and ventricular remodelling. *Cardiovasc. Res.* 27:145–57.
- Soonpaa MH, Field LJ. (1998) Survey of studies examining mammalian cardiomyocyte DNA synthesis. *Circ. Res.* 83:15–26.
- Buerke M, et al. (1995) Cardioprotective effect of insulin-like growth factor I in myocardial ischemia followed by reperfusion. *Proc. Natl. Acad. Sci. U. S. A.* 92:8031–5.
- Leri A, et al. (1999) Insulin-like growth factor-1 induces Mdm2 and down-regulates p53, attenuating the myocyte renin-angiotensin system and stretch-mediated apoptosis. *Am. J. Pathol.* 154:567–80.
- Li Q, et al. (1997) Overexpression of insulin-like growth factor-1 in mice protects from myocyte death after infarction, attenuating ventricular dilation, wall stress, and cardiac hypertrophy. *J. Clin. Invest.* 100:1991–9.
- Wang L, Ma W, Markovich R, Chen JW, Wang PH. (1998) Regulation of cardiomyocyte apoptotic signaling by insulin-like growth factor I. *Circ. Res.* 83:516–22.
- Anversa P, Nadal-Ginard B. (2002) Cardiac chimerism: methods matter. *Circulation* 106:e129–31.
- Chew SL, Lavender P, Clark AJ, Ross RJ. (1995) An alternatively spliced human insulin-like growth factor-I transcript with hepatic tissue expression that diverts away from the mitogenic IBE1 peptide. *Endocrinology* 136:1939–44.
- Yang S, Alnaqeeb M, Simpson H, Goldspink G. (1996) Cloning and characterization of an IGF-1 isoform expressed in skeletal muscle subjected to stretch. *J. Muscle Res. Cell Motil.* 17:487–495.
- Gilmour RS. (1994) The implications of insulin-like growth factor mRNA heterogeneity. *J. Endocrinol.* 140:1–3.
- Shavlakadze T, Winn N, Rosenthal N, Grounds MD. (2005) Reconciling data from transgenic mice that overexpress IGF-I specifically in skeletal muscle. *Growth Horm. IGF. Res.* 15:4–18.
- Pfeffer MA, et al. (1979) Myocardial infarct size and ventricular function in rats. *Circ. Res.* 44:503–12.
- Tenta R, Sourla A, Lembessis P, Koutsilieris M. (2006) Bone-related growth factors and zole-dronic acid regulate the PTHrP/PTH.1 receptor bioregulation systems in MG-63 human osteosarcoma cells. *Anticancer Res.* 26:283–91.
- Bickel CS, Slade JM, Haddad F, Adams GR, Dudley GA. (2003) Acute molecular responses of skeletal muscle to resistance exercise in able-bodied and spinal cord-injured subjects. *J. Appl. Physiol.* 94:2255–62.
- Kim JS, Cross JM, Bamman MM. (2005) Impact of resistance loading on myostatin expression and cell cycle regulation in young and older men and women. *Am. J. Physiol. Endocrinol. Metab.* 288: E1110–9.
- Philippou A, et al. (2008) Characterization of a rabbit antihuman mechano growth factor (MGF) polyclonal antibody against the last 24 amino acids of the E domain. *In Vivo* 22:27–35.
- Koutsilieris M, Rabbani SA, Bennett HP, Goltzman D. (1987) Characteristics of prostate-derived growth factors for cells of the osteoblast phenotype. *J. Clin. Invest.* 80:941–6.
- Papageorgiou E, Pitulis N, Manoussakis M, Lembessis P, Koutsilieris M. (2008) Rosiglitazone attenuates insulin-like growth factor 1 receptor survival signaling in PC-3 cells. *Mol. Med.* 14:403–11.
- LeRoith D, Werner H, Beitner-Johnson D, Roberts CT Jr. (1995) Molecular and cellular aspects of the insulin-like growth factor I receptor. *Endocr. Rev.* 16:143–63.
- Denley A, Cosgrove LJ, Booker GW, Wallace JC, Forbes BE. (2005) Molecular interactions of the IGF system. *Cytokine Growth Factor Rev.* 16:421–39.
- Adams GR. (2002) Invited review: autocrine/paracrine IGF-I and skeletal muscle adaptation. *J. Appl. Physiol.* 93:1159–67.
- Philippou A, Halapas A, Maridaki M, Koutsilieris M. (2007) Type I insulin-like growth factor receptor signaling in skeletal muscle regeneration and hypertrophy. *J. Musculoskelet. Neuronal Interact.* 7:208–18.
- Coolican SA, Samuel DS, Ewton DZ, McWade FJ, Florini JR. (1997) The mitogenic and myogenic actions of insulin-like growth factors utilize distinct signaling pathways. *J. Biol. Chem.* 272:6653–62.
- Dolcet X, Egea J, Soler RM, Martin-Zanca D, Comella JX. (1999) Activation of phosphatidylinositol 3-kinase, but not extracellular-regulated kinases, is necessary to mediate brain-derived neurotrophic factor-induced motoneuron survival. *J. Neurochem.* 73:521–31.
- Carpenter V, et al. (2008) Mechano-growth factor reduces loss of cardiac function in acute myocardial infarction. *Heart Lung Circ.* 17:33–9.
- Stanton LW, et al. (2000) Altered patterns of gene expression in response to myocardial infarction. *Circ. Res.* 86:939–45.
- Lee WL, Chen JW, Ting CT, Lin SJ, Wang PH. (1999) Changes of the insulin-like growth factor I system during acute myocardial infarction: implications on left ventricular remodeling. *J. Clin. Endocrinol. Metab.* 84:1575–81.
- Blankesteijn WM, et al. (2001) Dynamics of cardiac wound healing following myocardial infarction: observations in genetically altered mice. *Acta Physiol. Scand.* 173:75–82.
- Fedak PW, Verma S, Weisel RD, Skrtic M, Li RK. (2005) Cardiac remodeling and failure: from molecules to man (part III). *Cardiovasc. Pathol.* 14:109–19.
- Cleutjens JP, Blankesteijn WM, Daemen MJ, Smits JF. (1999) The infarcted myocardium: simply dead tissue, or a lively target for therapeutic interventions. *Cardiovasc. Res.* 44:232–41.
- Harpster MH, et al. (2006) Earliest changes in the left ventricular transcriptome postmyocardial infarction. *Mamm. Genome* 17:701–15.
- Pfeffer MA, Braunwald E. (1990) Ventricular remodeling after myocardial infarction: experimental observations and clinical implications. *Circulation* 81:1161–72.
- Chien KR, Knowlton KU, Zhu H, Chien S. (1991) Regulation of cardiac gene expression during myocardial growth and hypertrophy: molecular studies of an adaptive physiologic response. *FASEB J.* 5:3037–46.
- Sugden PH, Clerk A. (1998) Cellular mechanisms of cardiac hypertrophy. *J. Mol. Med.* 76:725–46.
- Adams GR. (2002) Autocrine and/or paracrine insulin-like growth factor-I activity in skeletal muscle. *Clin. Orthop. Relat. Res.* S188–96.
- Yang H, Alnaqeeb M, Simpson H, Goldspink G. (1997) Changes in muscle fibre type, muscle mass and IGF-I gene expression in rabbit skeletal muscle subjected to stretch. *J. Anat.* 190 (Pt 4): 613–22.
- Musaro A, et al. (2001) Localized Igf-1 transgene expression sustains hypertrophy and regeneration in senescent skeletal muscle. *Nat. Genet.* 27:195–200.
- Rosenthal N, Musaro A. (2002) Gene therapy for cardiac cachexia? *Int. J. Cardiol.* 85:185–91.
- Reiss K, et al. (1994) Acute myocardial infarction leads to upregulation of the IGF-1 autocrine system, DNA replication, and nuclear mitotic division in the remaining viable cardiac myocytes. *Exp. Cell Res.* 213:463–72.
- Reiss K, et al. (1996) Overexpression of insulin-like growth factor-1 in the heart is coupled with myocyte proliferation in transgenic mice. *Proc. Natl. Acad. Sci. U. S. A.* 93:8630–5.
- DeLaughter MC, Taffet GE, Fiorotto ML, Entman ML, Schwartz RJ. (1999) Local insulin-like growth factor I expression induces physiologic, then pathologic, cardiac hypertrophy in transgenic mice. *FASEB J.* 13:1923–9.
- Duerr RL, et al. (1995) Insulin-like growth factor-1 enhances ventricular hypertrophy and function during the onset of experimental cardiac failure. *J. Clin. Invest.* 95:619–27.
- Saetrum Opgaard O, Wang PH. (2005) IGF-I is a matter of heart. *Growth Horm. IGF. Res.* 15:89–94.
- Li B, et al. (1999) Insulin-like growth factor-1 attenuates the detrimental impact of nonocclusive coronary artery constriction on the heart. *Circ. Res.* 84:1007–19.
- Wu W, et al. (2000) Expression of constitutively active phosphatidylinositol 3-kinase inhibits activation of caspase 3 and apoptosis of cardiac muscle cells. *J. Biol. Chem.* 275:40113–9.
- Parrizas M, Blakesley VA, Beitner-Johnson D, LeRoith D. (1997) The proto-oncogene Crk-II enhances apoptosis by a Ras-dependent, Raf-1/MAP kinase-independent pathway. *Biochem. Biophys. Res. Commun.* 234:616–20.
- Ren J, Samson WK, Sowers JR. (1999) Insulin-like growth factor I as a cardiac hormone: physiological and pathophysiological implications in heart disease. *J. Mol. Cell Cardiol.* 31:2049–61.
- Foncea R, et al. (2000) Extracellular regulated kinase, but not protein kinase C, is an antiapop-

- totic signal of insulin-like growth factor-1 on cultured cardiac myocytes. *Biochem. Biophys. Res. Commun.* 273:736–44.
49. Fujio Y, Nguyen T, Wencker D, Kitsis RN, Walsh K. (2000) Akt promotes survival of cardiomyocytes in vitro and protects against ischemia-reperfusion injury in mouse heart. *Circulation* 101:660–7.
 50. Cook SA, Matsui T, Li L, Rosenzweig A. (2002) Transcriptional effects of chronic Akt activation in the heart. *J Biol. Chem.* 277:22528–33.
 51. Padmasekar M, Nandigama R, Wartenberg M, Schluter KD, Sauer H. (2007) The acute phase protein alpha2-macroglobulin induces rat ventricular cardiomyocyte hypertrophy via ERK1,2 and PI3-kinase/Akt pathways. *Cardiovasc. Res.* 75:118–28.
 52. Kim J, *et al.* (2008) Insulin-like growth factor I receptor signaling is required for exercise-induced cardiac hypertrophy. *Mol. Endocrinol.* 22:2531–43.
 53. Molkenin JD, Dorn GW 2nd. (2001) Cytoplasmic signaling pathways that regulate cardiac hypertrophy. *Annu. Rev. Physiol.* 63:391–426.
 54. Clerk A, Gillespie-Brown J, Fuller SJ, Sugden PH. (1996) Stimulation of phosphatidylinositol hydrolysis, protein kinase C translocation, and mitogen-activated protein kinase activity by bradykinin in rat ventricular myocytes: dissociation from the hypertrophic response. *Biochem. J.* 317:109–18.
 55. Thorburn J, *et al.* (1995) Inhibition of a signaling pathway in cardiac muscle cells by active mitogen-activated protein kinase kinase. *Mol. Biol. Cell* 6:1479–90.
 56. Thorburn J, Xu S, Thorburn A. (1997) MAP kinase- and Rho-dependent signals interact to regulate gene expression but not actin morphology in cardiac muscle cells. *EMBO J.* 16:1888–1900.
 57. Post GR, Goldstein D, Thuerauf DJ, Glembotski CC, Brown JH. (1996) Dissociation of p44 and p42 mitogen-activated protein kinase activation from receptor-induced hypertrophy in neonatal rat ventricular myocytes. *J Biol. Chem.* 271:8452–7.
 58. Tolis G, *et al.* (1983) Suppression of testicular steroidogenesis by the GnRH agonistic analogue Buserelin (HOE-766) in patients with prostatic cancer: studies in relation to dose and route of administration. *J. Steroid Biochem.* 19:995–8.
 59. Koutsilieris M, Allaire-Michaud L, Fortier M, Lemay A. (1991) Mitogen(s) for endometrial-like cells can be detected in human peritoneal fluid. *Fertil. Steril.* 56:888–93.
 60. Koutsilieris M. (1992) Pathophysiology of uterine leiomyomas. *Biochem. Cell Biol.* 70:273–8.
 61. Sourla A, Doillon C, Koutsilieris M. (1996) Three-dimensional type I collagen gel system containing MG-63 osteoblasts-like cells as a model for studying local bone reaction caused by metastatic cancer cells. *Anticancer Res.* 16:2773–80.
 62. Koutsilieris M, Mitsiades C, Sourla A. (2000) Insulin-like growth factor I and urokinase-type plasminogen activator bioregulation system as a survival mechanism of prostate cancer cells in osteoblastic metastases: development of anti-survival factor therapy for hormone-refractory prostate cancer. *Mol. Med.* 6:251–67.
 63. Mitsiades CS, Koutsilieris M. (2001) Molecular biology and cellular physiology of refractoriness to androgen ablation therapy in advanced prostate cancer. *Expert Opin. Investig. Drugs* 10:1099–115.